Supporting Information for

Copper Vulcanization Realizes Selective Carbon Dioxide Reduction to Formate

Wenqiang Liu[a],[#] Yan Wen[a],[#] Nan Fang[a], Mingmin Wang[a], Yong Xu[b],[*], and Xiaoqing Huang[a],[*]

[a]State Key Laboratory of Physical Chemistry of Solid Surfaces, College of Chemistry and Chemical Engineering, Xiamen University, Xiamen, 361005, China. E-mail: hxq006@xmu.edu.cn

[b]Guangzhou Key Laboratory of Low-Dimensional Materials and Energy Storage Devices, Collaborative Innovation Center of Advanced Energy Materials, School of Materials and Energy, Guangdong University of Technology, Guangzhou, 510006, China. E-mail: yongxu@gdut.edu.cn

1. Experimental Section

1.1 Chemicals.

Cuprous thiocyanate (CuSCN, 99%), cupric acetate (Cu(HCOO)$_2$, 99%), and cupric acetate (Cu(HCOO)$_2$, 99%) were purchased from Macklin, Walk World, and 3 A, respectively. Copper sulfate (CuSO$_4$, 99%), ethanol (C$_6$H$_6$O$_2$, analytical reagent, ≥99.7%), cyclohexane (C$_6$H$_{12}$, analytical reagent, ≥99.7%), N,N-dimethylformamide (DMF), hydrazine hydrate (N$_2$H$_4$·H$_2$O, 85%), ammonium hydroxide (NH$_3$·H$_2$O, 28%) and potassium hydroxide (KOH, 85 %) were supplied by Sinopharm Chemical Reagent Co. Ltd. (Shanghai, China). Polyvinylpyrrolidone K30-K33 (PVP) and thioacetamide (TAA, 99%) were obtained from Anegi, while oleylamine (OAm) was provided by Aladdin. All chemical reagents were used as received without further purification. All aqueous solutions were prepared using deionized water with a resistivity of 18.2 MΩ cm.

1.2 Synthesis of Cu$_2$S nanosheets (NSs).

For the synthesis of Cu$_2$S NSs, 30 mg CuSCN was dissolved in 5 mL OAm with ultrasonication for 1 h. The mixture was then heated in an oil bath at 180 °C for 2h. The cooled product was collected by centrifugation and washed three times with a mixture of cyclohexane/ethanol (v/v = 1:9).

1.3 Synthesis of Cu NSs and Cu+S NSs.

For the synthesis of Cu+S NSs, 30 mg Cu(HCOO)$_2$ and 300 mg PVP was dissolved in 15 mL DMF with ultrasonication for 1 h. The mixture was then heated in an oil bath at 40 °C for 10 min. Afterwards, 90 μL of hydrazine hydrate was added drop by drop to the vessel and heated in an oil bath at 60 °C for 30 min. Lastly, adding 22.5 mg TAA into the vessel and heated at 80 °C for 30 min to get Cu+S nanosheet. The preparation process of Cu NSs follows Cu+S NSs without adding TAA. The cooled product was collected by centrifugation and washed for three times with ethanol/acetone (v/v = 1:9) mixture.

1.4 Synthesis of CuO NSs and CuO+S NSs.

In a typical synthesis of CuO+S NSs, 100 mg CuSO$_4$ was dissolved in 4 mL deionized water, and 2.5 mL KOH (1 M) solution was then added dropwise into the solution. After stirring for 15 min, 1 mL NH$_3$·H$_2$O ws added. The resulting homogeneous light blue solution was then transferred to a glass pressure vessel. The sealed vessel was then heated from room temperature to 80 °C in 30 min and kept for 12 h. Afterwards, 60 mg TAA was added into the vessel at 80 °C for 1 h to get CuO+S NSs. The preparation process of CuO NSs was similar to that of CuO+S NSs except for the absence of TAA. After cooling to room temperature, the product was collected by centrifugation and washed three times with deionized water.

1.5 Synthesis of Cu(OH)$_2$ NSs and Cu(OH)$_2$+S NSs.

For the synthesis of Cu(OH)$_2$+S NSs, 100 mg CuSO$_4$ was dissolved in 6.5 mL deionized water, and 2.5 mL KOH (1 M) solution was then dropwise added into the solution. After stirring for 15 min, 1 mL NH$_3$·H$_2$O was added into the mixed solution, and was then transferred to a glass vessel. Finally, 1 mL TAA solution (0.1 M) was added into the vessel and with ultrasonication for 1 h to get Cu(OH)$_2$+S NSs. The preparation process of Cu(OH)$_2$ NSs was similar to that of Cu(OH)$_2$+S NSs except for the absence of sodium sulfide solution. The finally product was collected by centrifugation and washed three times with deionized water.

1.6 Characterizations.

XRD measurement was conducted on a SmartLab-SE powder diffractometer equipped with a Cu radiation source ($\lambda = 0.15406$ nm). SEM-EDS was performed by a ZEISS Sigma 300 field emission scanning electron microscope. TEM was operated on JEM-1400 TEM at an accelerating voltage of 100 kV. HRTEM was conducted on a FEI Tecnai F30 TEM at an accelerating voltage of 300 kV. HAADF-STEM-EDS was conducted on a FEI Titan Cubed Themis G2300. The X-ray photoelectron spectroscopy spectra were collected by XPS (Thermo Scientific, ESCALAB 250 XI). The carbon peak at 284.8 eV was used as the reference to correct for charging effects. Raman spectra were characterized by Renishaw RT 1000. The concentrations of the catalysts were determined by ICP-OES (ICAP 7000, ThermoFisher, USA). Electrochemical in situ Attenuated Total Reflection Flourier Transformed Infrared Spectroscopy (ATR-FTIR) was employed to trace the signals of the intermediates using a Nicolet Nexus 670 Spectroscopy equipped with a liquid nitrogen-cooled mercury-cadmium-telluride (MCT) detector. An ECIR-II cell equipped with a Pike Veemax III ATR in a three-electrode system was provided from Shanghai Linglu Instrument& Equipment Co. The monocrystal silicon was initially coated with a layer of Au to improve the signal intensity.

1.7 CO_2 Electroreduction in H-Cell.

Three-electrode system was used to perform the electrochemical CO_2 reduction in H cell. A micro Ag/AgCl electrode (4.0 M KCl) and a Pt wire were used as reference electrode and counter electrode, respectively. The catalyst ink was prepared by ultrasonicating 10 mg of catalyst with 500 μL isopropanol, 450 μL H_2O and 50 μL of 5 wt % Nafion solutions for 1 h. A 100 μL suspension was then deposited on carbon paper (1 x 1 cm^2) to prepare the working electrodes. Electrochemical reduction of CO_2 was conducted in a gastight H-cell separated by a cation exchange membrane (Nafion117) on a CHI660 (Chenhua, Shanghai) electrochemical workstation. Each chamber contained 20 mL 0.1 M $KHCO_3$ aqueous solution with a 30 mL headspace. As for the electrochemical measurements, the CO_2 was delivered into the cathodic compartment (directly connected to gas chromatograph (GC Agilent 7890B) at a constant rate of 20 sccm and was allowed to purge for 30 min prior to the beginning of experiments. Then, the reactions were tested by the chronoamperometry method under different potentials. The gas phase composition was analyzed by GC equipped with a PLOT MolSieve5A column and a Q-bond PLOT column every 15 min with different potentials applied. Liquid products were characterized by 1 H NMR on Agilent 600 MHz DirectDrive2 spectrometers. 1 H chemical shifts were referenced to residual protic solvent signals. All potentials were given against the reversible hydrogen electrode (RHE), calculated using the Nernst equation without ohmic IR drop correction. The faradaic efficiency (FE) for the formation of a hydrocarbon was calculated as follows: $FE = eF \times n/Q = eF \times n/(I \times t)$, where e is the number of electrons transferred, F is the Faraday constant, Q is the charge, I is the current, t is the running time, and n is the total amount of product (in moles).

1.8 CO_2 Electroreduction in Flow Cell.

Electroreduction was performed in a flow cell configuration that consisted of a catalyst-deposited gas diffusion electrode (GDE) as the working electrode, an anion-exchange membrane (Fumasep FAB-PK-130), and Pt foil as the anode. GDEs were prepared by loading catalysts onto a gas diffusion layer (Catalysts' ink was prepared by mixing 4.5 mg catalyst, 10 μL of 5 wt % Nafion solutions, and 1 mL of ethanol. The ink was sonicated for 20 min before loading. The GDE with catalysts, anion exchange membrane and Pt foil were then positioned and clamped together using polytetrafluoroethylene spacers. Thus, a liquid electrolyte could be introduced into the chambers between the anode and membrane as well as between the membrane and cathode. Gaseous CO_2 was then passed behind the gas diffusion layer to diffuse into the liquid electrolyte presented at the catalytic area (0.5 × 2 cm^2). In the catholyte stream, a port drilled into the polytetrafluoro-ethylene spacer allowed a micro reference Ag/AgCl electrode (4.0 M KCl) to be positioned at a specific distance from the working electrode. All the electrochemical experiments were performed using a CHI660 (Chenhua, Shanghai) electrochemical

workstation with a current amplifier. The electrolyte (1 M KOH solution, 20 mL for each of the catholyte and anolyte) was circulated through the electro-chemical cell using peristaltic pumps. The electrolyte flow was kept at 40 mL min^{-1}. CO_2 flow was kept constant at 30 mL min^{-1} with a mass flow controller. The reactions were tested by chronopotenti-ometry method at different currents for 20 min without ohmic IR drop correction. Prior to CO_2RR, Cu_2S/C was electrochemically activated at 250 mA·cm^{-2} for 100 min, which was named as Cu_2S/C-A. The methods for analyzing liquid and gaseous products in flow cell were the same as those in H cell.
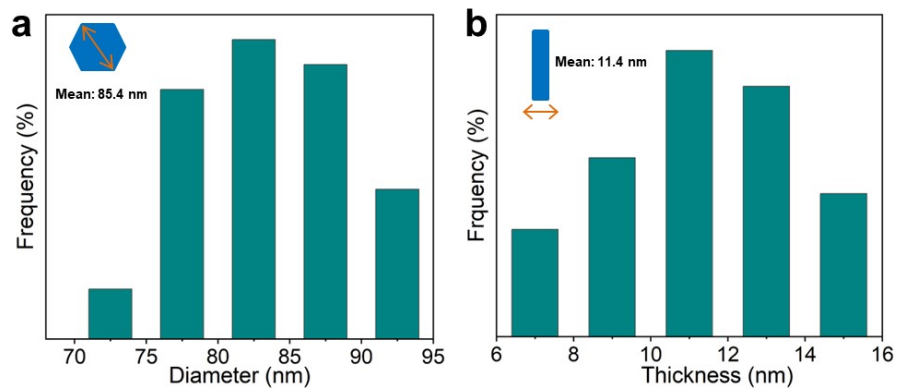
Figure S1. (a) Diameter distribution and (b) thickness distribution of Cu$_2$S NSs.
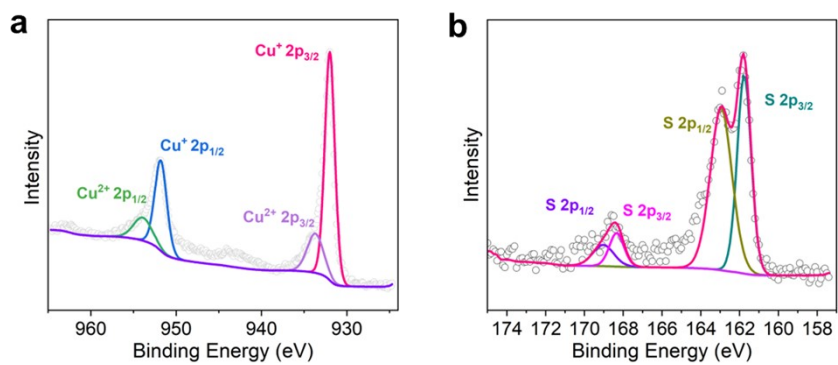
Figure S2. (a) Cu 2p and (b) S 2p XPS spectra of Cu_2S NSs.
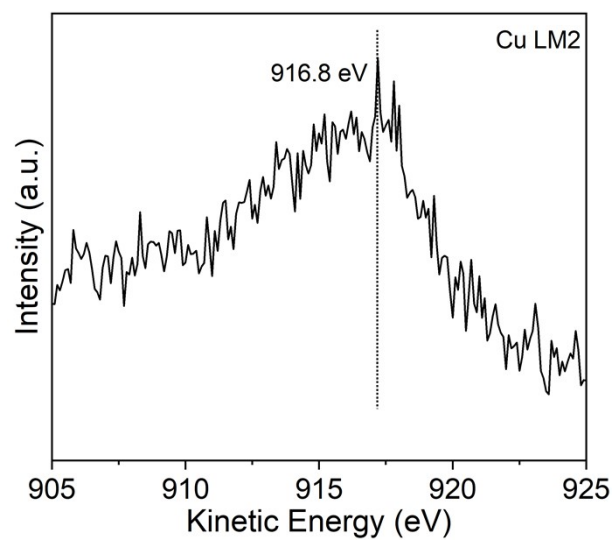
Figure S3. Cu LM2 XPS spectrum of Cu_2S NSs. The peak at 916.8 eV was ascribed to Cu^+.
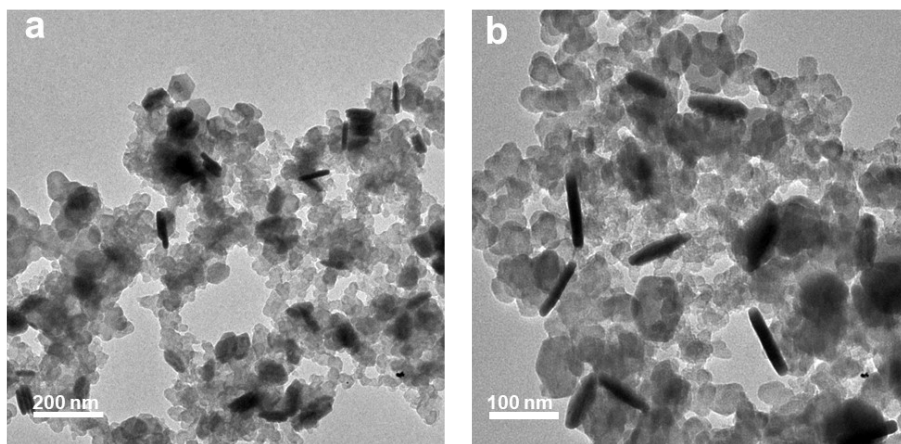
Figure S4. (a, b) TEM images of Cu$_2$S/C.
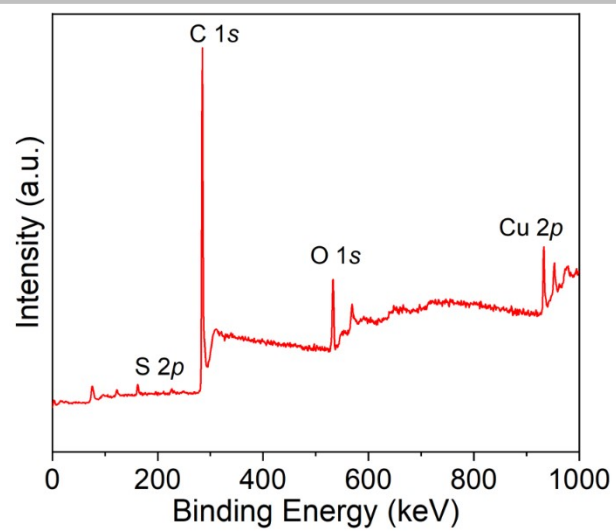
Figure S5. XPS survey spectra of Cu_2S/C.
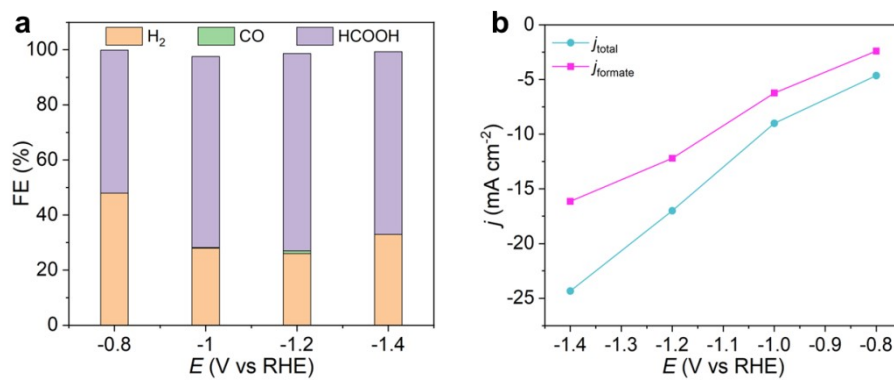
Figure S6. CO$_2$RR performance over Cu$_2$S/C in H-cell. (a) FEs of products at given potentials, and (b) corresponding current densities for formate and total products.
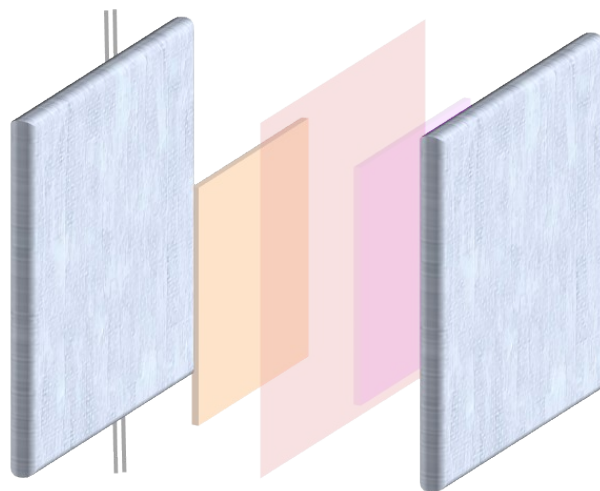
Figure S7. Schematic illustration of the flow cell configuration.
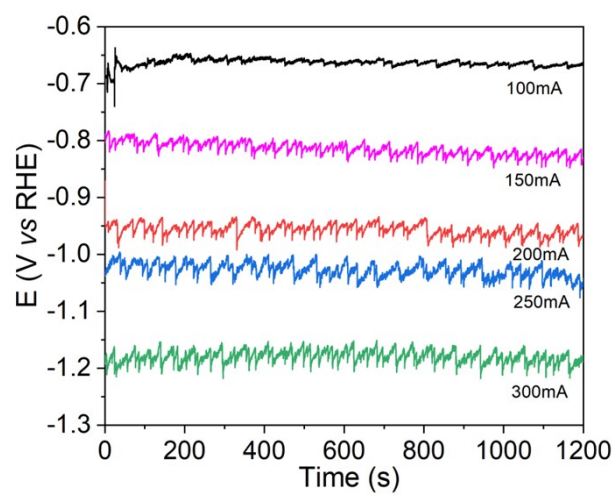
Figure S8. Chronopotentiometry curves of Cu$_2$S/C under different applied currents.
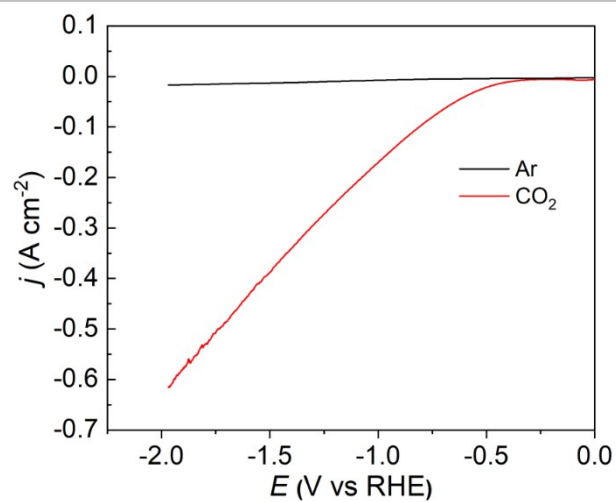
Figure S9. LSV curves of Cu_2S/C. The polarized curves were collected in a conventional three-electrode flow-cell system at a scan rate of 0.1 V s $^{-1}$. The values of potential were presented without iR compensation.
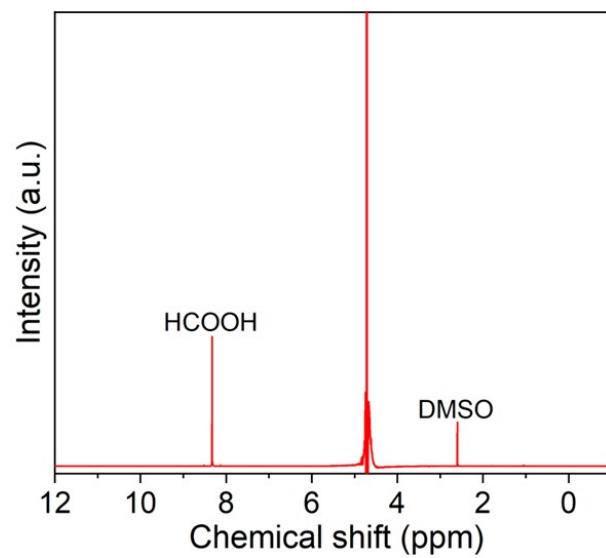
Figure S10. H-NMR spectra of liquid products for CO$_2$RR at -1.06 vs. RHE over Cu$_2$S/C.
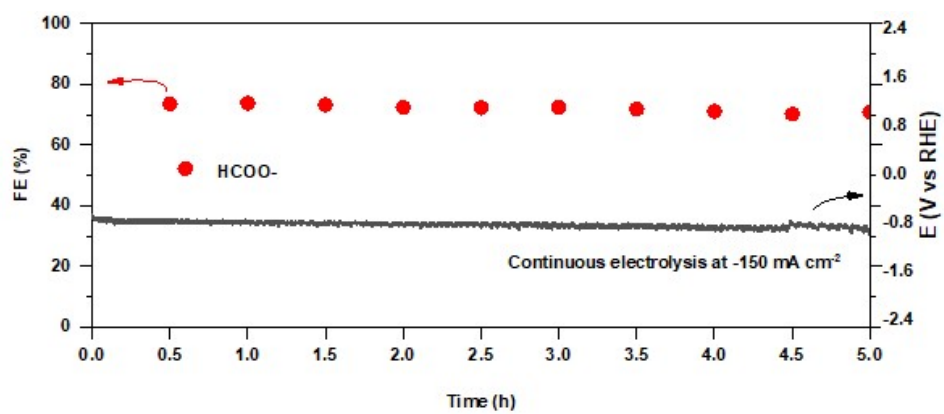
Figure S11. Stability test of the Cu$_2$S at 150 mA·cm^{-2}.
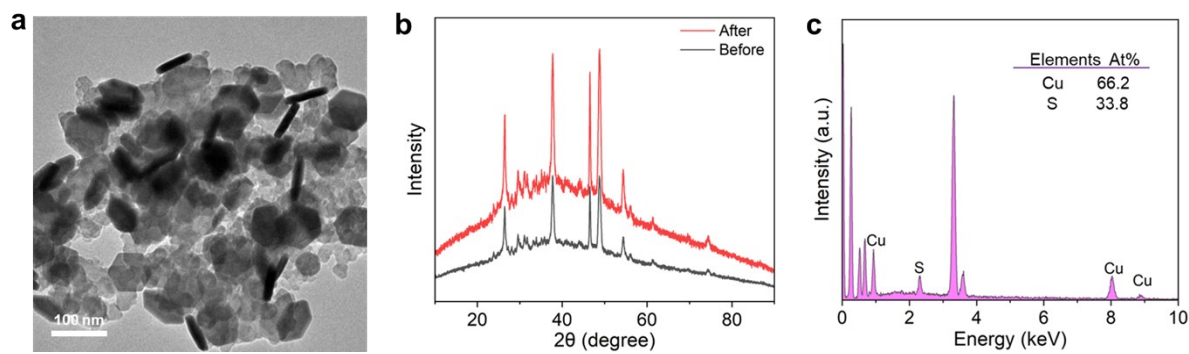
Figure S12. (a) TEM image of Cu_2S/C after the CO_2RR test at 150 mA·cm^{-2}, (b) XRD pattern of Cu_2S/C before and after the CO_2RR test at 150 mA·cm^{-2}, (c) SEM-EDS spectrum of Cu_2S/C after the CO_2RR test at 150 mA·cm^{-2}.
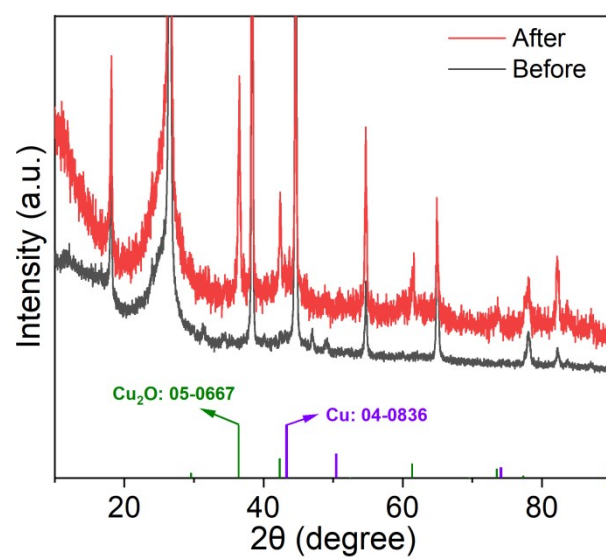
Figure S13. XRD pattern of Cu$_2$S/C before and after electroreduction.
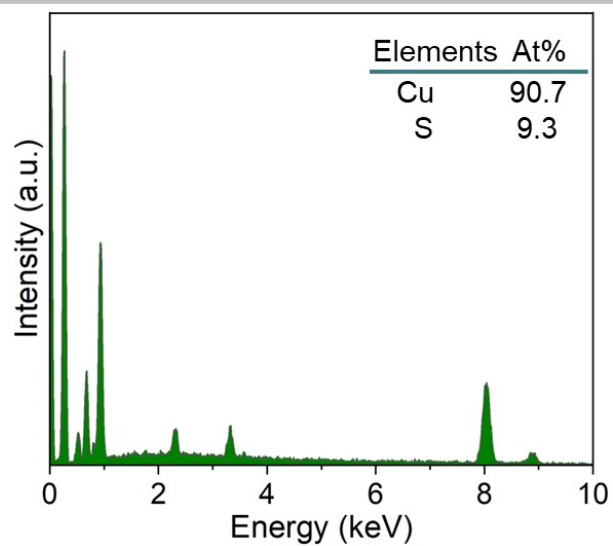
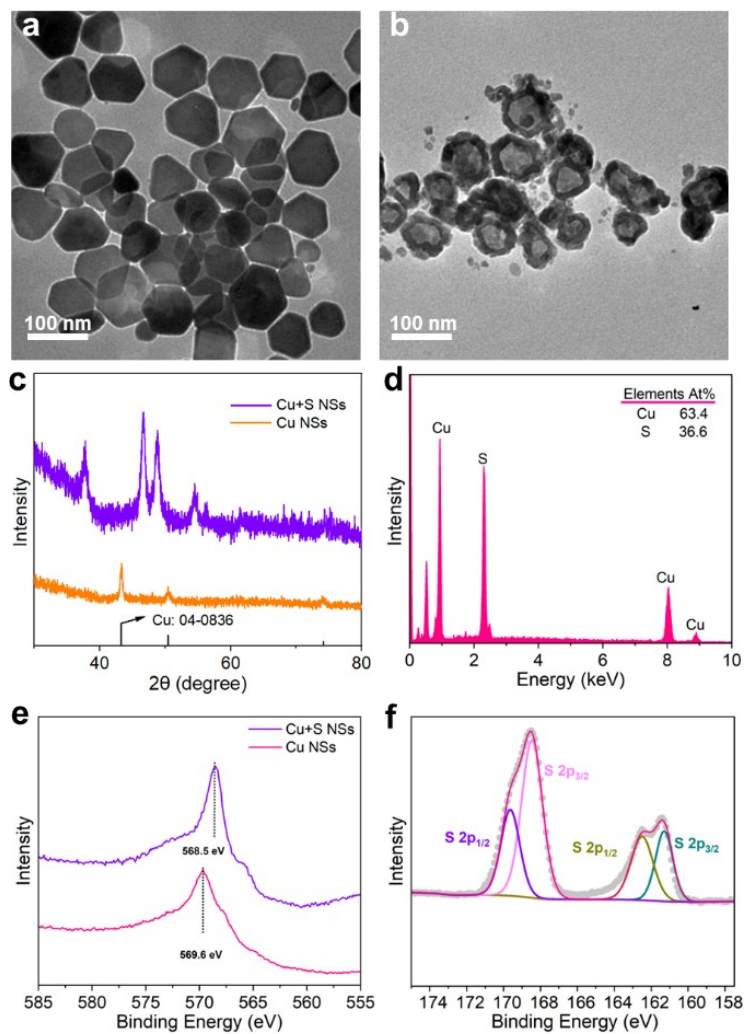**Figure S14.** SEM-EDS spectrum of Cu$_2$S/C after electroreduction.

Figure S15. TEM images of (a) Cu NSs and (b) Cu+S NSs. (c) XRD patterns of Cu NSs and Cu+S NSs. (d) SEM-EDS spectrum of Cu+S NSs. (e) Cu LM2 XPS spectrum of Cu NSs and Cu+S NSs. (f) S 2p XPS spectrum of Cu+S NSs.
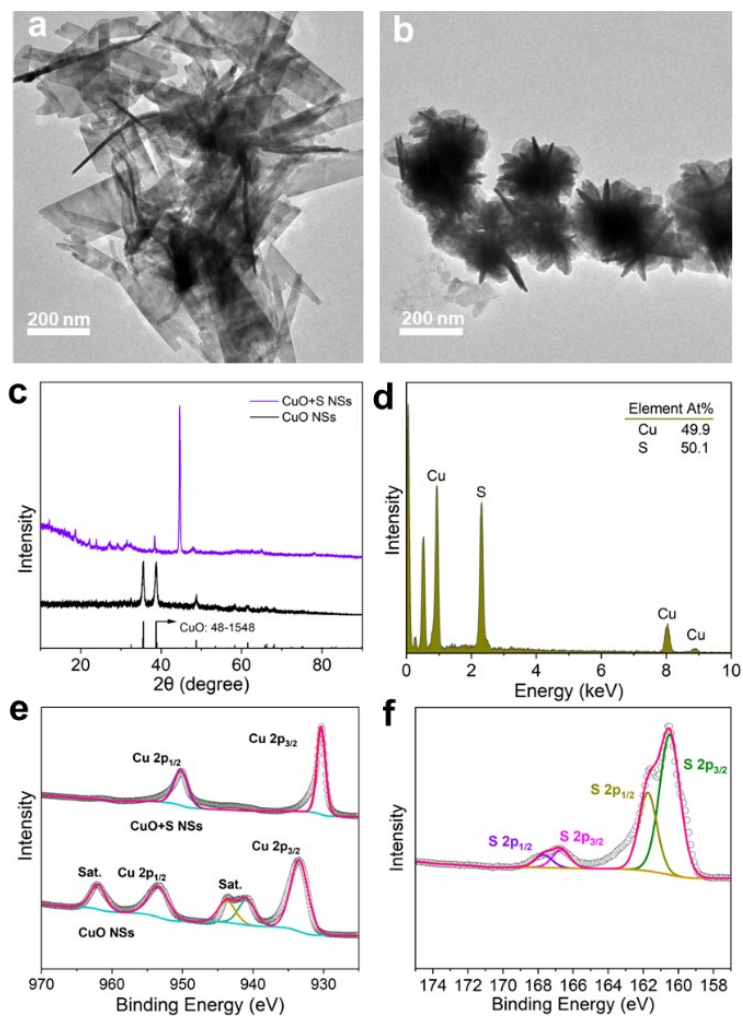
Figure S16. TEM images of (a) CuO NSs and (b) CuO+S NSs. (c) XRD patterns of CuO NSs and CuO+S NSs. (d) SEM-EDS spectrum of CuO+S NSs. (e) Cu XPS spectrum of CuO NSs and CuO+S NSs. (f) S 2p XPS spectrum of CuO+S NSs.
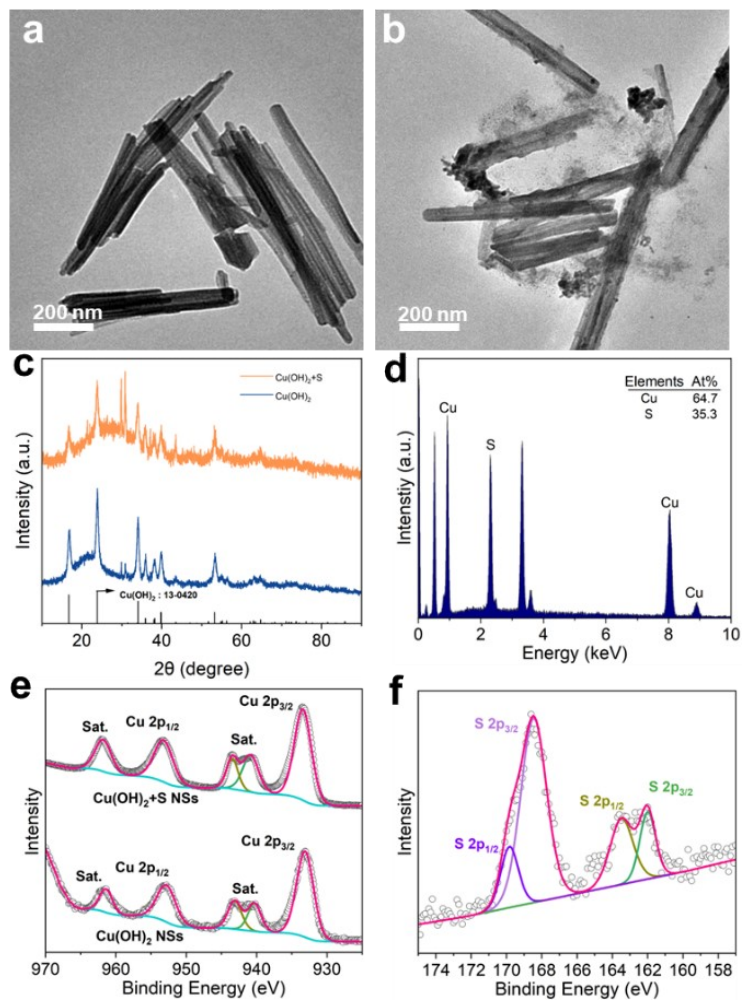
Figure S17. TEM images of (a) Cu(OH)$_2$ NSs and (b) Cu(OH)$_2$+S NSs. (c) XRD patterns of Cu(OH)$_2$ NSs and Cu(OH)$_2$+S NSs. (d) SEM-EDS spectrum of Cu(OH)$_2$+S NSs. (e) Cu XPS spectrum of Cu(OH)$_2$ NSs and Cu(OH)$_2$+S NSs. (f) S 2p XPS spectrum of Cu(OH)$_2$+S NSs.
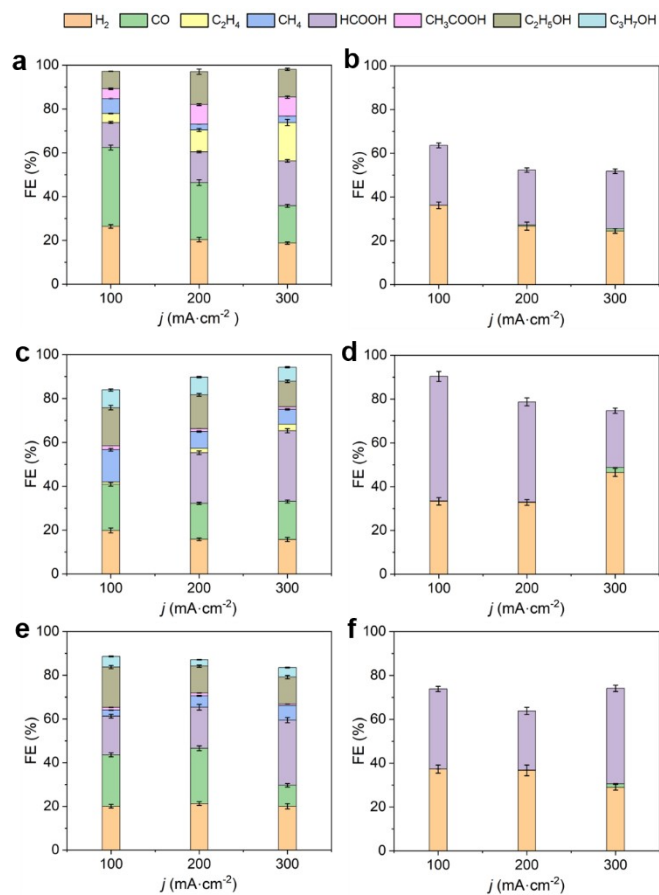
Figure S18. CO_2RR performances in flow cell. FEs of products at different current densities of (a) Cu NS and (b) Cu+S NS, (c) CuO NS and (d) CuO+S NS, (e) $Cu(OH)_2$ NS and (f) $Cu(OH)_2$+S NS.

Table S1. The potentials of Cu_2S/C vs. Ag/AgCl reference electrode.[a]

j_{total} (mA cm^{-2})	E (V vs Ag/AgCl)	E (V vs RHE)
100	-1.71	-0.70
150	-1.86	-0.84
200	-2.00	-0.99
250	-2.08	-1.06
300	-2.23	-1.21

[a]: The potentials vs. RHE were calculated based on the equation: E (vs. RHE) = E (vs Ag/AgCl) + 0.197 + (0.0595 x pH) without iR correction.